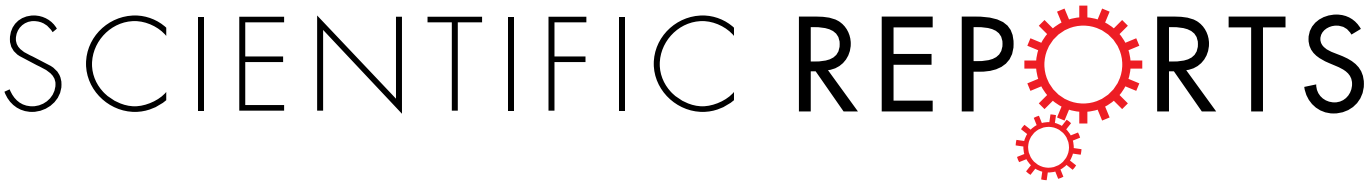

OPEN

Optical properties of drug metabolites in latent fingermarks

Yao Shen[1] & Qing Ai[2]

Received: 14 October 2015
Accepted: 30 December 2015
Published: 03 February 2016

Drug metabolites usually have structures of split-ring resonators (SRRs), which might lead to negative permittivity and permeability in electromagnetic field. As a result, in the UV-vis region, the latent fingermarks images of drug addicts and non drug users are inverse. The optical properties of latent fingermarks are quite different between drug addicts and non-drug users. This is a technic superiority for crime scene investigation to distinguish them. In this paper, we calculate the permittivity and permeability of drug metabolites using tight-binding model. The latent fingermarks of smokers and non-smokers are given as an example.

In 1968, negative index material (NIM) was first introduced by Veselago[1]. NIM can have negative permittivity and permeability simultaneously. Pendry *et al.*[2–6] gave a deep discussion and pointed out that a configuration which was called split-ring resonator (SRR)[3] could put negative refraction into practice, apart from some particular configurations with non-trivial symmetry breaking[7]. From then on, negative refraction became a focus in scientific research, for example NIM can be used to fabricate perfect lenses to enhance local field and detection sensitivity[8–11]. Two years later, Shelby *et al.*[12] realized NIM experimentally. Metamaterial, made up of SRRs or molecules which consist of SRRs, e.g. extended metal atom chains, becomes a new branch of study[13–37]. Many new directions are developed, such as electromagnetic cloaking[38–43], toroidal moment[44], liquid crystal magnetic control[45], etc. On the other hand, in forensic science, on highly reflective surface, the latent fingermarks are difficult to be observed. The traditional method of visualizing the invisible fingermarks is using fluorescent tag. In Boddis and Russell's paper[46], they made use of antibody-magnetic particle conjugates to visualize them. During this procedure, they find the latent fingermarks of smokers and non-smokers are quite different. As a result, the latent fingermarks of these two kinds of donors are observed to be inverse and thus they can be used to identify the smokers. The research of distinguishing drug users by metabolites becomes a new focus in forensic science field[47,48]. In this paper, we first introduce negative refraction phenomenon to forensic science. We point out that when we put those latent fingermarks of drug addicts and non-drug users in the light field, they can also be identified. Furthermore, our method is physical and non-damaged, because the latent fingermarks will not be destroyed. More importantly, due to quantum effect, a small volume of molecules could sufficiently respond negatively to the applied electromagnetic fields[49]. We give the theoretical derivation and calculation of this phenomenon. Our result is not only suitable for smokers but also for drug addicts. In other words, except for cotinine, the metabolite of nicotine, benzoylecgonine and morphine can also be detected using our method.

Results

Tight-binding Approximation and Hückel Model. Many molecules of drug metabolites have a broken ring configuration, i.e. SRR. This structure gives them special optical properties. Without loss of generality, we calculate cotinine, i.e. the metabolite of nicotine, as an example.

Figure 1(a) demonstrates the structure of cotinine molecule. The main part of cotinine is the hexagon part which is called pyridine as shown in Fig. 1(b). In this part, one carbon atom of the ring is substituted with one nitrogen atom. For the sake of simplicity, the remaining part of cotinine molecule is simplified as a methyl in the same plane. This simplification is reasonable because the main contribution to the optical property comes from the π electrons in the conjugate part of cotinine molecule, i.e. single-nitrogen-substituted heterocyclic annulene[50] or 3-methylpyridine in Fig. 1(c). Hückel calculation is justifiable and sufficient for the 3-methylpyridine model, though it is a simplified model. Recently, by using a small set of empirical parameters, the Hückel method has been successfully applied to calculate the energy of highest-occupied π orbital and the first $\pi - \pi^*$ transition energy for a large set of organic molecules with less than 13% deviation. As a consequence, we utilize the Hückel model with the set of empirical parameters to simulate the optical properties of cotinine molecules in our paper.

[1]School of Forensic Science, People's Public Security University of China, Beijing 100038, China. [2]Department of Physics, Applied Optics Beijing Area Major Laboratory, Beijing Normal University, Beijing 100875, China. Correspondence and requests for materials should be addressed to Y.S. (email: shenyaophysics@hotmail.com)

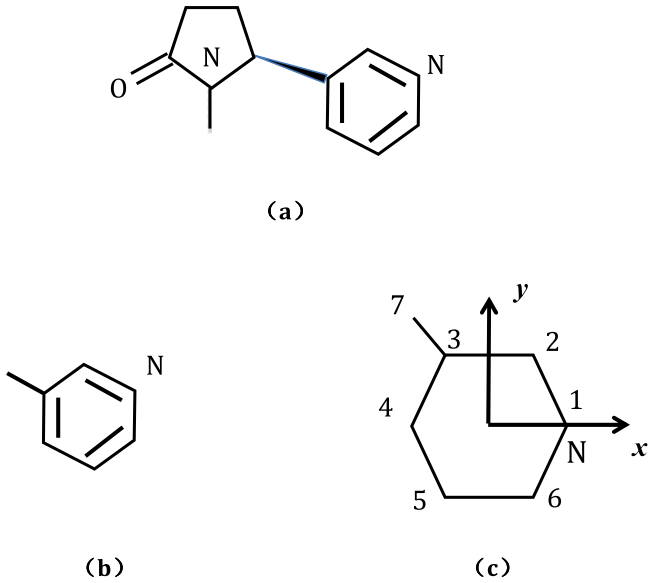

Figure 1. (**a**) The chemical structure of cotinine molecule ($C_{10}H_{12}N_2O$). Cotinine has two rings, one is pyridyl, and the other is pyrrolidine. (**b**) The simplified model. The molecule is simplified into a pyridyl and a methyl. (**c**) The spatial distribution of atoms in the simplified model. The origin is set at the center of the hexagon. Seven sites are labeled sequentially. Site 1 is a nitrogen atom and others are carbon atoms.

Alternatively, we also notice that by taking σ orbital into account, extended Hückel theory[51–54] may provide better result with much less consuming time as compared to other more accurate method, e.g. time-dependent density function theory.

π electrons of the pyridyl interact with the electromagnetic fields and therefore result in special optical properties of cotinine. The structure of 3-methylpyridine consists of one pyridyl and one methyl with sites labeled as in Fig. 1(c). Although there are seven electrons in 3-methylpyridine, it has been discovered that one of the electrons is mainly located at the methyl and does not contribute to the current in the ring. Because the magnetic response originates from the circular current, hereafter we shall restrict our calculation to the pyridyl. However, due to the presence of methyl, two carbon-carbon bond lengths have been slightly modified. The problem starts from toluene (methylbenzene) which adds a methyl on a benzene. The quantum dynamics of six π electrons of benzene are described by the Hückel model as[55]

$$H^{benzene} = \sum_{j=1}^{6} \alpha_j |j\rangle\langle j| + \sum_{j=1}^{6} \beta_{j,j+1}(|j\rangle\langle j+1| + |j+1\rangle\langle j|), \tag{1}$$

where j is the site label, $|j\rangle$ denotes the state with a π electron at site j, α_j is the site energy and $\alpha_C = -6.7\,eV$[56]. The coupling strength between jth and $(j+1)$th sites is given by the resonant integral $\beta_{j,j+1} = \beta_{CC} = -2.462\,eV$. Here we use Harrison expression[57,58]

$$\beta_{ij} = -0.63\frac{\hbar^2}{m_e d_{ij}^2}, \tag{2}$$

where $\hbar$ is the Planck constant, m_e is the mass of electron, d_{ij} is the bond length and can be attained from NIST[56,59]. Benzene has four energy levels ε_1, ε_2, ε_3, ε_4, which are labeled sequentially from the lowest eigen energy. Both the degeneracies of ε_2 and ε_3 are two, while ε_1 and ε_4 are non-degenerate.

For toluene, the resonant integrals of benzene have been modified, because the bond lengths are revised by the presence of the methyl. The bond length of benzene is $d = 1.397\,A$, while toluene have two values, i.e. $d_1 = 1.394\,A$ and $d_2 = 1.395\,A$[56,59]. The smaller one is the bond length between carbon which is connected to the methyl and its adjacent atoms. The revised resonant integrals are $\beta_1 = -2.469\,eV$ and $\beta_2 = -2.473\,eV$. As labeled in Fig. 1(c), the Hückel Hamiltonian of toluene reads

$$\begin{aligned} H^{toluene} = & \sum_{j=1}^{6} \alpha_C |j\rangle\langle j| + \sum_{j=1,4,5,6} \beta_1(|j\rangle\langle j+1| + |j+1\rangle\langle j|) \\ & + \beta_2(|2\rangle\langle 3| + |3\rangle\langle 2| + |3\rangle\langle 4| + |4\rangle\langle 3|). \end{aligned} \tag{3}$$

In this case, the energy spectrum of toluene can be solved exactly as

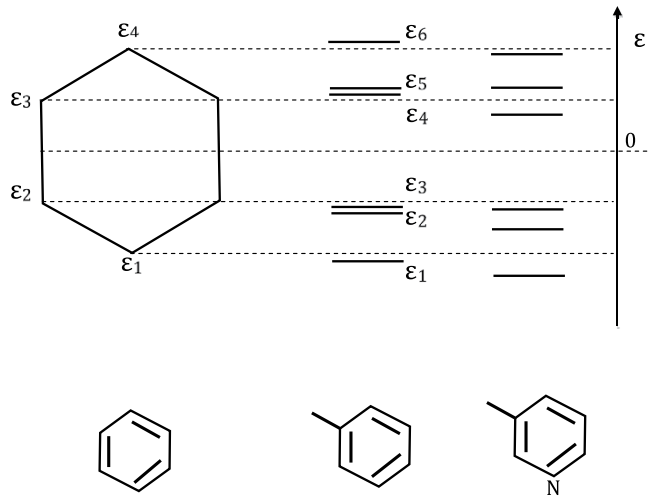

Figure 2. The energy spectra of (left) benzene, (middle) toluene and (right) simplified cotinine molecule.

$$\begin{aligned}
\varepsilon_1 &= \frac{1}{2}\left(2\alpha_C - \sqrt{2}\sqrt{3\beta_1^2 + 2\beta_2^2 + \sqrt{9\beta_1^4 - 4\beta_1^2\beta_2^2 + 4\beta_2^4}}\right) = \alpha_C - 4.941\,eV,\\
\varepsilon_2 &= \frac{1}{2}\left(2\alpha_C - \sqrt{2}\sqrt{3\beta_1^2 + 2\beta_2^2 - \sqrt{9\beta_1^4 - 4\beta_1^2\beta_2^2 + 4\beta_2^4}}\right) = \alpha_C - 2.472\,eV,\\
\varepsilon_3 &= \alpha_C + \beta_1 = \alpha_C - 2.469\,eV,\\
\varepsilon_4 &= \alpha_C - \beta_1 = \alpha_C + 2.469\,eV,\\
\varepsilon_5 &= \frac{1}{2}\left(2\alpha_C + \sqrt{2}\sqrt{3\beta_1^2 + 2\beta_2^2 - \sqrt{9\beta_1^4 - 4\beta_1^2\beta_2^2 + 4\beta_2^4}}\right) = \alpha_C + 2.472\,eV,\\
\varepsilon_6 &= \frac{1}{2}\left(2\alpha_C + \sqrt{2}\sqrt{3\beta_1^2 + 2\beta_2^2 + \sqrt{9\beta_1^4 - 4\beta_1^2\beta_2^2 + 4\beta_2^4}}\right) = \alpha_C + 4.941eV,
\end{aligned} \tag{4}$$

which are schematically shown in Fig. 2. And we do not list the eigen vectors here for simplicity. Because of the methyl, the degeneracy is lifted.

For simplified cotinine, the Hamiltonian is described as

$$H = \sum_{j=1}^{6}\alpha_j|j\rangle\langle j| + \sum_{j=1}^{6}\beta_{j,j+1}(|j\rangle\langle j+1| + |j+1\rangle\langle j|). \tag{5}$$

The nitrogen atom is located at site 1, cf. Fig. 1(c). In this configuration, the site energies and coupling constants are explicitly given as

$$\alpha_j = \begin{cases} \alpha_C = -6.7\,eV, \text{ for } j \neq 1, \\ \alpha_N = -7.9\,eV, \text{ for } j = 1, \end{cases} \tag{6}$$

$$\beta_{j,j+1} = \begin{cases} \beta_1, \text{ for } j = 4,5, \\ \beta_2, \text{ for } j = 2,3, \\ \beta_{CN} = -2.676\,eV\,(d_{CN} = 1.34A), \text{ for } j = 1,6. \end{cases} \tag{7}$$

By diagonalization, the Hückel Hamiltonian (5) can be reexpressed as

$$H = \sum_{k=1}^{6}\varepsilon_k|\psi_k\rangle\langle\psi_k|, \tag{8}$$

where $|\psi_k\rangle = \sum_{j=1}^{6} C_{kj}|j\rangle$ is kth single-electron molecular orbital, ε_k is the eigen energy.

In order to obtain $|\psi_k\rangle$ and ε_k, we use the perturbation theory in quantum mechanics. We assume that the unperturbed system is a toluene. Then, the perturbation originates from

$$H' = H - H^{toluene} = (\alpha_N - \alpha_C)a_1^\dagger a_1 + (\beta_{CN} - \beta_1)(a_1^\dagger a_2 + a_2^\dagger a_1 + a_1^\dagger a_6 + a_6^\dagger a_1), \tag{9}$$

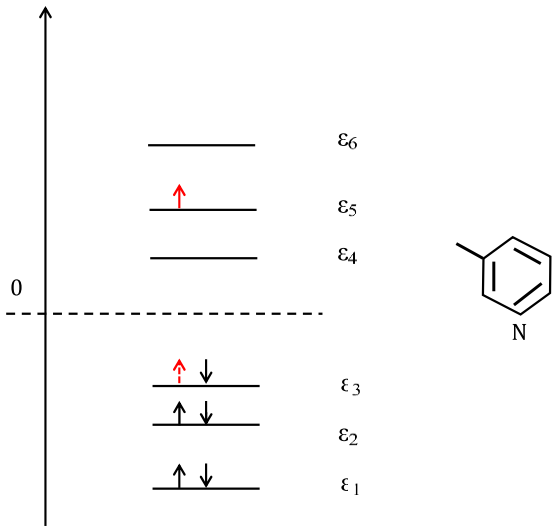

Figure 3. Schematic for the single-electron excitation of cotinine molecule (red solid up-arrow) from the ground state (red dashed up-arrow), i.e. $|\Psi_0\rangle \rightarrow |\Psi_3\rangle$ with transition energy $\Delta E_3 = E_3 - E_0 = \varepsilon_5 - \varepsilon_3$.

where $a_j^\dagger$ is the creation operator on jth site and a_j is the annihilation operator. As a consequence, the simplified cotinine molecule has also six energy levels (see Fig. 2), and all of them are non-degenerate. Hereafter, for the sake of simplicity, we further assume $\alpha_C = 0$.

According to the perturbation theory, the energy spectrum of the simplified cotinine molecule reads

$$\begin{aligned} &\varepsilon_1 = -5.384eV,\ \varepsilon_2 = -2.956eV,\ \varepsilon_3 = -2.471eV,\ \varepsilon_4 = +2.245eV, \\ &\varepsilon_5 = +2.471eV,\ \varepsilon_6 = +4.895eV. \end{aligned} \tag{10}$$

Following the degenerate perturbation theory, we can obtain the wave function to the first order. Since their explicit expressions are very complicated, we do not list the analytical expressions of energy and wave function here.

The cotinine molecule has six non-interacting π-electrons. On account of the spin degree (see Fig. 3), the ground state can be expressed in the second-quantization form as

$$|\Psi_0\rangle = a_{1\uparrow}^\dagger a_{1\downarrow}^\dagger a_{2\uparrow}^\dagger a_{2\downarrow}^\dagger a_{3\uparrow}^\dagger a_{3\downarrow}^\dagger |0\rangle, \tag{11}$$

and E_0 represents the ground-state energy of the whole cotinine system, i.e.

$$E_0 = 2(\varepsilon_1 + \varepsilon_2 + \varepsilon_3), \tag{12}$$

where $a_{k\sigma}^\dagger$ is the creation operator of the orbital k with spin $\sigma(\sigma = \uparrow, \downarrow)$.

The system has eighteen single-excitation states, for example, the 2th and 3th excited states are

$$|\Psi_2\rangle = a_{1\uparrow}^\dagger a_{1\downarrow}^\dagger a_{2\uparrow}^\dagger a_{2\downarrow}^\dagger a_{3\uparrow}^\dagger a_{4\downarrow}^\dagger |0\rangle,\ |\Psi_3\rangle = a_{1\uparrow}^\dagger a_{1\downarrow}^\dagger a_{2\uparrow}^\dagger a_{2\downarrow}^\dagger a_{5\uparrow}^\dagger a_{3\downarrow}^\dagger |0\rangle,$$

with corresponding eigen energies

$$E_2 = 2(\varepsilon_1 + \varepsilon_2) + \varepsilon_3 + \varepsilon_4,\ E_3 = 2(\varepsilon_1 + \varepsilon_2) + \varepsilon_3 + \varepsilon_5,$$

respectively. In the first case, the electron with energy ε_3 and spin down is excited to energy level ε_4 with spin conserved. In the second case, the electron with energy ε_3 and spin up is excited to energy level ε_5 with spin conserved. Here the flip of electronic spin is not taken into consideration. To sum up, the single-excitation states read

$$|\Psi_n\rangle = \left|\Psi_{p\sigma}^{q\sigma}\right\rangle = a_{q\sigma}^\dagger a_{p\sigma} |\Psi_0\rangle, \tag{13}$$

where $p = 1, 2, 3$, $q = 4, 5, 6$, $\sigma = \uparrow, \downarrow$, and the eigen energies are

$$E_n = E_0 + \varepsilon_q - \varepsilon_p. \tag{14}$$

In the subspaces spanned by the ground state and single-excitation states, the Hamiltonian without electro-magnetic field reads

$$\mathcal{H}_0 = \sum_{n=0}^{18} E_n |\Psi_n\rangle\langle\Psi_n|. \tag{15}$$

Perturbation Theory in Electromagnetic Field. When there is a time-dependent electromagnetic field applied on the molecule, based on the dipole approximation, the total Hamiltonian including the interaction between the molecule and the electromagnetic field can be written as

$$\begin{aligned}\mathcal{H} &= \mathcal{H}_0 - \vec{\mu}\cdot\vec{E}(\vec{r},t) - \vec{m}\cdot\vec{B}(\vec{r},t)\\ &\simeq \mathcal{H}_0 - \vec{\mu}\cdot\vec{E}_0\ \cos(\vec{k}\cdot\vec{r}-\omega t) - \vec{m}\cdot\vec{B}_0\ \cos(\vec{k}\cdot\vec{r}-\omega t),\end{aligned} \tag{16}$$

where $\overrightarrow{\mu}$ and $\overrightarrow{m}$ denote the electric and magnetic dipole moments respectively. By assuming the spatial scale of the molecule is much smaller than the wave length of the field $\vec{k}\cdot\vec{r}\simeq 0$ since the coordinate is chosen as Fig. 1(c), we have

$$\mathcal{H}\simeq\mathcal{H}_0 - \vec{\mu}\cdot\vec{E}_0\ \cos(\omega t) - \vec{m}\cdot\vec{B}_0\ \cos(\omega t). \tag{17}$$

By a unitary transformation

$$U^\dagger = \exp(-i\omega t|\Psi_0\rangle\langle\Psi_0|), \tag{18}$$

the Hamiltonian becomes time-independent

$$\begin{aligned}\mathcal{H}' &= U^\dagger\mathcal{H}U - iU^\dagger\dot{U}\\ &\simeq \sum_{n=1}^{18}E_n|\Psi_n\rangle\langle\Psi_n| + (E_0+\omega)|\Psi_0\rangle\langle\Psi_0| + \mathcal{H}'',\end{aligned} \tag{19}$$

where

$$\begin{aligned}\mathcal{H}'' &= -\frac{1}{2}\sum_{n=1}^{18}(\vec{\mu}_{n0}\cdot\vec{E}_0|\Psi_n\rangle\langle\Psi_0| + \vec{\mu}_{0n}\cdot\vec{E}_0|\Psi_0\rangle\langle\Psi_n|)\\ &\quad -\frac{1}{2}\sum_{n=1}^{18}(\vec{m}_{n0}\cdot\vec{B}_0|\Psi_n\rangle\langle\Psi_0| + \vec{m}_{0n}\cdot\vec{B}_0|\Psi_0\rangle\langle\Psi_n|),\end{aligned} \tag{20}$$

$$\vec{\mu}_{nn'} = \langle\Psi_n|\vec{\mu}|\Psi_{n'}\rangle, \tag{21}$$

$$\vec{m}_{nn'} = \langle\Psi_n|\vec{m}|\Psi_{n'}\rangle. \tag{22}$$

In other words, we change the system from the static frame into a rotating frame. In the rotating frame, the state and operator become $|\Psi'\rangle = U^\dagger|\Psi\rangle$, and $A' = U^\dagger AU$, respectively. Moreover, due to the interaction with electromagnetic field, the molecular ground state becomes

$$|\Psi_0'\rangle = U^\dagger|\Psi_0\rangle = |\Psi_0\rangle + \sum_{n=1}^{18}\frac{\langle\Psi_n|H''|\Psi_0\rangle}{E_0+\omega-E_n}|\Psi_n\rangle, \tag{23}$$

Permittivity. The electric dipole moment in the rotating frame reads

$$\vec{\mu}' = U^\dagger\vec{\mu}U = \sum_{n=1}^{18}(\vec{\mu}_{n0}e^{i\omega t}|\Psi_n\rangle\langle\Psi_0| + \vec{\mu}_{0n}e^{-i\omega t}|\Psi_0\rangle\langle\Psi_n|). \tag{24}$$

For the ground state, the expectation value for the dipole operator in the rotating frame is

$$\langle\Psi_0'|\vec{\mu}'|\Psi_0'\rangle = -\,Re\sum_{n=1}^{18}\frac{\vec{\mu}_{n0}\cdot\vec{E}_0}{E_0+\omega-E_n}\vec{\mu}_{0n}e^{-i\omega t}. \tag{25}$$

In the electromagnetic field, the electric displacement field in a volume V with N identical molecules

$$\vec{D} = \varepsilon\vec{E}_0 = \varepsilon_0\varepsilon_r\vec{E}_0 = \varepsilon_0\vec{E}_0 + \frac{\vec{P}}{V} \tag{26}$$

reads

$$\vec{D} = \varepsilon_0\vec{E}_0 - \sum_{s=1}^{N}\sum_{n=1}^{18}\frac{[\vec{\mu}_{n0}(s)\cdot\vec{E}_0]\vec{\mu}_{0n}(s)}{V(E_0+\omega-E_n)}. \tag{27}$$

Thus, the total permittivity in different direction is

$$\varepsilon_{ij} = \varepsilon_0\delta_{ij} - \sum_{s=1}^{N}\sum_{n=1}^{18}\frac{\mu_{0n}^{(i)}(s)\mu_{n0}^{(j)}(s)}{(E_0+\omega-E_n)V}, \text{ for } i, j = x, y, z \tag{28}$$

The relative dielectric constant of the system, i.e. the permittivity, gives

$$\varepsilon_{ij}^{r} \equiv \delta_{ij} - \sum_{s=1}^{N}\sum_{n=1}^{18}\frac{\vec{\mu}_{0n}(s)\cdot\hat{e}_i\vec{\mu}_{n0}(s)\cdot\hat{e}_j}{\varepsilon_0 V(E_0+\omega-E_n)}, \text{ for } i, j = x, y, z, \tag{29}$$

where $\hat{e}_i$ is the unit vector of the lab coordinate system.

Because we choose the symmetric center of pyridyl as the origin of coordinate, the electric dipole moment reads

$$\vec{\mu} = -\sum_{j=1}^{6} e\vec{r}_j, \tag{30}$$

where $\vec{r}_j$ is the vector of jth electron and $-e$ is the electric charge of an electron. Because $\vec{r}_j$'s are single-electron operators, the matrix elements of electric dipole operators are given by

$$\vec{\mu}_{0n} = \langle\Psi_0|\vec{\mu}|\Psi_n\rangle = -e\langle\Psi_0|\vec{r}|\Psi_n\rangle = -e\langle\psi_p\left|\vec{r}\right|\psi_q\rangle = -e\vec{r}_{pq}, \tag{31}$$

where $\vec{r}_{pq}$ is the overlap of $\vec{r}$ between two single-electron wave functions, i.e.

$$\langle\psi_p\left|\vec{r}\right|\psi_q\rangle = \sum_{j=1}^{6} C_{pj}^{*}C_{qj}\vec{r}_j. \tag{32}$$

Permeability. To account for the magnetic response of cotinine molecule, we start from the Heisenberg equations of motion,

$$p^x = m_e\dot{r}^x = im_e[\mathcal{H}, r^x], \tag{33}$$

$$p^y = m_e\dot{r}^y = im_e[\mathcal{H}, r^y], \tag{34}$$

where we assume $\hbar = 1$.

The magnetic dipole moment is related to the angular momentum of the system. The angular momentum operators read

$$L_x = r^y p^z - r^z p^y = 0, \tag{35}$$

$$L_y = r^z p^x - r^x p^z = 0, \tag{36}$$

$$L_z = r^x p^y - r^y p^x = \frac{1}{2}(r^x p^y + p^y r^x - r^y p^x - p^x r^y) = im_e(r^x\mathcal{H}r^y - r^y\mathcal{H}r^x). \tag{37}$$

Obviously, only the response in z direction is present as all atoms in the cotinine molecule are restricted in the xy plane. Therefore, the magnetic dipole moment is

$$\vec{m} = \frac{-e}{2m_e}\vec{L} = \frac{-e}{2m_e}L_z\hat{e}_z = \frac{-ie}{2}(r^x\mathcal{H}r^y - r^y\mathcal{H}r^x)\hat{e}_z = \frac{-ie}{2}\sum_{k,k'}\sum_{n}E_n(r_{kn}^x r_{nk'}^y - r_{kn}^y r_{nk'}^x)|\Psi_k\rangle\langle\Psi_{k'}|\hat{e}_z, \tag{38}$$

where

$$r_{kk'}^{\alpha} = \langle\psi_k|r^{\alpha}|\psi_{k'}\rangle. \tag{39}$$

Similar to the electric response, the expectation value for the magnetic dipole operator in the rotating frame is

$$\langle\Psi_0'|\vec{m}'|\Psi_0'\rangle = -Re\sum_{n=1}^{18}\frac{\vec{m}_{n0}\cdot\vec{B}_0}{E_0+\omega-E_n}\vec{m}_{0n}e^{-i\omega t}. \tag{40}$$

The magnetic induction in a volume V with N identical molecules

$$\vec{B} = \mu\vec{H}_0 = \mu_0\mu_r\vec{H}_0 = \mu_0\vec{H}_0 + \mu_0\frac{\vec{M}}{V} \tag{41}$$

is explicitly given by

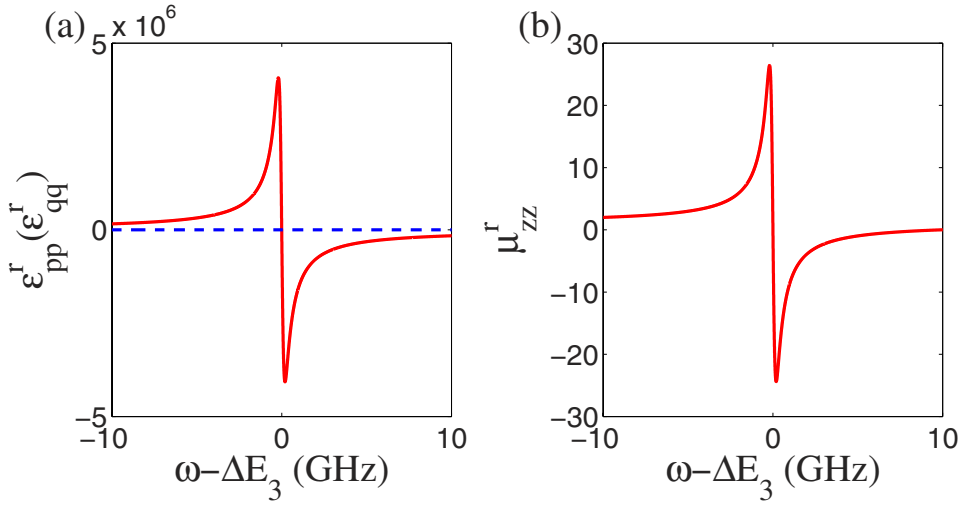

Figure 4. The numerical results of (a) permittivity and (**b**) permeability of cotinine molecules vs the light frequency ω. The permittivity ε^r_{oo} (red solid line) along one main axis in the xy plane is negative near the resonance frequency, while ε^r_{pp} (blue dashed line) along the other main axis is always constant. In the magnetic response, the permeability along z direction μ^r_{zz} is shown.

$$\vec{B} = \mu_0 \vec{H}_0 - \sum_{s=1}^{N}\sum_{n=1}^{18} \frac{\mu_0 \vec{m}_{n0}(s) \cdot \vec{B}_0}{V(E_0 + \omega - E_n)} \vec{m}_{0n}(s). \tag{42}$$

Notice that μ is the permeability of medium, different from the electric dipole moment $\vec{\mu}$ above.

The relative permeability of cotinine medium is simplified as

$$\mu^r_{ij} \equiv \delta_{ij} - \mu_0 \sum_{s=1}^{N}\sum_{n=1}^{18} \frac{\vec{m}_{0n}(s) \cdot \hat{e}_i \vec{m}_{n0}(s) \cdot \hat{e}_j}{V(E_0 + \omega - E_n)}, \text{ for } i, j = x, y, z. \tag{43}$$

Analysis. Equations (29) and (43) present the analytical results for the relative permittivity and permeability of cotinine molecules in electromagnetic field. According to the expressions of these two quantities, they can be negative simultaneously when the second parts of the expressions are greater than unity. In order to fulfill this requirement, the denominators of the second parts should be small enough. In other words, $E_0 + \omega - E_n$ needs to be much smaller than numerator which means $\omega \approx E_n - E_0$. For a given initial energy of the electron before transition E_0, we can observe simultaneous negative permittivity and permeability of cotinine molecules in electromagnetic field when the driving frequency ω is tuned approximately equal to the transition frequency $E_n - E_0$.

Numerical Simulation of Permittivity and Permeability. In the above section, the analytical derivation suggests that relative permittivity and permeability of cotinine molecules might be negative simultaneously in certain frequency regime. Here we show and analyze the numerical result. In the investigated model, the cotinine molecule is simplified as a pyridine and a methyl, c.f. Fig. 1(b). The simplified cotinine model is of two dimension. Thus, we only need to analyze the electromagnetic responses of the molecules in two directions. Figure 4 shows the numerical simulation of relative dielectric constants in the xy plane and relative magnetic permittivity in z direction of the system. Here we assume the site energies $\alpha_C = 0$, $\alpha_N = \alpha_C - 1.2\,eV$, and the coupling strengths $\beta_{CC} = -2.462$ eV, revised coupling strengths $\beta_1 = -2.469$ eV, $\beta_2 = -2.473$ eV, $\beta_{CN} = -2.676\,eV$[55,57–59]. The excited-state life time $\tau = 10$ ns is within the range of experimentally observation, e.g. 90 μs[60]. For a transition to the first excited state, e.g. a spin-up electron is excited from ε_3 to ε_4, the contributions from transition dipoles μ_{01} and m_{01} are much larger than others i.e., $\omega \sim \Delta E_3 = \varepsilon_5 - \varepsilon_3$. In Fig. 4(a), both relative dielectric constants in the two main axes ε^r_{pp} and ε^r_{qq} are different from unity in the vacuum case, as the presence of nitrogen atom breaks the reflection symmetry along the axis connecting site 3 and the origin. Furthermore, Fig. 4 clearly shows the negative permittivity and permeability at the same time. This result suggests that cotinine molecules can be detected by negative refraction.

Discussion

In this paper we research the optical properties of drug metabolites in latent fingermarks. All of these drug metabolites have a structure in common, i.e. SRR which could realize negative refraction. And negative refraction makes the optical properties of latent fingermark quite different between drug addicts and non-drug users and thus can be used to distinguish them. Illuminated by the same incident field, the latent fingermarks of these two kinds of donors may be observed in the different directions with respect to the normal of the interface. The method is to print the donor's fingermarks on the transparent media and to observe them in the light transmission direction

on the opposite side with respect to the side for the normal refraction. In the ordinary case, the refracted light and incident light are on the opposite sides of the normal. However, if the donor is a drug addict, we can detect the refracted light on the same side of incident light with respect to the normal. Although the concentration of drug metabolites may not be evenly distributed in the fingermark, some parts of the fingermark can be detected by negative refraction once the concentrations of drug metabolites in these parts are sufficiently large. Because of negative refraction, the fingermarks of drug addicts can be distinguished from those of non-drug users. Without loss of generality, we take cotinine as an example to calculate electromagnetic response of metabolites in latent fingermarks of smokers. According to our analytic derivation and numerical simulation, we demonstrate the presence of negative refraction in cotinine molecules. The advantage of this method is that it is physical and non-damaged. Our method is suitable for all drug metabolites which have the SRR structure. And this method can also be conveniently applied to distinguish drug addicts and non-drug users. For example, except for cotinine, benzoylecgonine and morphine can also be detected using our method.

References

1. Veselago, V. G. The electrodynamics of substances with simultaneously negative values of ε and μ. *Sov. Phys. Uspekhi* **10,** 509–514 (1968).
2. Pendry, J. B. Negative refraction makes a perfect lens. *Phys. Rev. Lett.* **85,** 3966–3969 (2000).
3. Pendry, J. B., Holden, A. J., Robbins, D. J. & Stewart, W. J. Magnetism from conductors and enhanced nonlinear phenomena. *IEEE Trans. Microwave Theory Tech*. **47,** 2075–2084 (1999).
4. Pendry, J. B., Holden, A. J., Stewart, W. J. & Youngs, I. Extremely low frequency plasmons in metallic mesostructures. *Phys. Rev. Lett.* **76,** 4773–4776 (1996).
5. Pendry, J. B., Holden, A. J., Robbins, D. J. & Stewart, W. J. Low frequency plasmons in thin-wire structures. *J. Phys. Condens. Matter* **10,** 4785–4809 (1998).
6. Luo, Y., Zhao, R. K., Fernandez-Dominguez, A. I., Stefan, A. M. & John, P. B. Harvesting light with transformation optics. *Sci. Chin. Inf. Sci*. **56,** 120401 (2013).
7. Fang, Y. N., Shen, Y., Ai, Q. & Sun, C. P. Negative refraction induced by Möbius topology. *Preprint arXiv*:1501.05729.
8. Cubukcu, E., Zhang, S., Park, Y.-S., Bartal, G. & Zhang, X. Split ring resonator sensors for infrared detection of single molecular monolayers. *Appl. Phys. Lett.* **95,** 043113 (2009).
9. Clark, A. W., Glidle, A., Cumming, D. R. S. & Cooper, J. M. Plasmonic split-ring resonators as dichroic nanophotonic {DNA} biosensors. *J. Am. Chem. Soc.* **131,** 176150–17619 (2009).
10. Pryce, I. M., Kelaita, Y. A., Aydin, K., Briggs, R. M. & Atwater, H. A. Compliant metamaterials for resonantly enhanced infrared absorption spectroscopy and refractive index sensing. *ACS Nano* **5,** 8167–8174 (2011).
11. Ma, C. B., Aguinaldo, R. & Liu, Z. W. Advances in the hyperlens. *Chin. Sci. Bull.* **55,** 2618–2624 (2010).
12. Shelby, R. A., Smith, D. R. & Schultz, S. Experimental verification of a negative index of refraction. *Science* **292,** 77–79 (2001).
13. Ropp, C. *et al.* Positioning and immobilization of individual quantum dots with nanoscale precision. *Nano Lett.* **10,** 4673–4679 (2010).
14. Smith, D. R., Pendry, J. B. & Wiltshire, M. C. K. Metamaterials and negative refractive index. *Science* **305,** 788–792 (2004).
15. Decker, M., Linden, S. & Wegener, M. Coupling effects in low-symmetry planar split-ring resonator arrays. *Opt. Lett.* **34,** 1579–1581 (2009).
16. Pryce, I. M., Aydin, K., Kelaita, Y. A., Briggs, R. M. & Atwater, H. A. Highly strained compliant optical metamaterials with large frequency tunability. *Nano Lett.* **10,** 4222–4227 (2010).
17. Chen, W. T. *et al.* Optical magnetic response of upright plasmonic molecules in 3D metamaterial. SPIE Newsroom **2011**.
18. Liu, N., Liu, H., Zhu, S. & Giessen, H. Stereometamaterials. *Nat. Photonics* **3,** 157–162 (2009).
19. Fleming, G. R. & Wolynes, P. G. Chemical dynamics in solution. *Phys. Today* **43,** 36–43 (1990).
20. Szabo, A. & Ostlund, N. S. *Modern quantum chemistry: Introduction to advanced electronic structure theory* (Dover, New York, 1996).
21. Greenwood, H. H. *Computing methods in quantum organic chemistry* (Wiley-Interscience, Germany, 1972).
22. Pantazis, D. A. & McGrady, J. E. A three-state model for the polymorphism in linear tricobalt compounds. *J. Am. Chem. Soc*. **128,** 4128–4135 (2006).
23. Pyrka, G. J., El-Mekki, M. & Pinkerton, A. A. Structure of the linear trinuclear copper complex, dichlorotetrakis-(di-2-pyridylamido) tricopper. *J. Chem. Soc., Chem. Commun*. 84–85 (1991).
24. Peng, S.-M. *et al.* One-dimensional metal string complexes. *J. Magn. Magn. Mater*. **209,** 80–83 (2000).
25. Tsai, T.-W., Huang, Q.-R., Peng, S.-M. & Jin, B.-Y. Smallest electrical wire based on extended metal-atom chains. *J. Phys. Chem. C* **114,** 3641–3644 (2010).
26. Chae, D.-H. *et al.* Vibrational excitations in single trimetal-molecule transistors. *Nano Lett*. **6,** 165–168 (2006).
27. Chen, I.-W. P. *et al.* Conductance and stochastic switching of ligand-supported linear chains of metal atoms. *Angew. Chem. Int. Edit*. **45,** 5814–5818 (2006).
28. Chen, C. C. *et al.* Fabrication of three dimensional split ring resonators by stress-driven assembly method. *Opt. Express* **20,** 9415–9420 (2012).
29. Ishikawa, A. & Tanaka, T. J. Two-photon fabrication of three-dimensional metallic nanostructures for plasmonic metamaterials. *Laser Micro Nanoeng*. **7,** 11–15 (2012).
30. Shen, Y. & Jin, B.-Y. Correspondence between Gentile oscillators and N-annulenes. *J. Phys. Chem. A* **117,** 12540–12545 (2013).
31. Shen, Y., Dai, W. S. & Xie, M. Intermediate-statistics quantum bracket, coherent state, oscillator, and representation of angular momentum [SU(2)] algebra. *Phys. Rev. A* **75,** 042111 (2007).
32. Shen, Y., Ai, Q. & Long, G. L. The relation between properties of Gentile statistics and fractional statistics of anyon. *Phys. A* **389,** 1565–1570 (2010).
33. Zhang, S. & Zhang, Y. Broadband unidirectional acoustic transmission based on piecewise linear acoustic metamaterials. *Chin. Sci. Bull*. **59,** 3239–3245 (2014).
34. Cao, J. J. *et al.* Dielectric optical-controllable magnifying lens by nonlinear negative refraction. *Sci. Rep*. **5,** 11892 (2015).
35. Philippe, F. D., Murray, T. W. & Prada, C. Focusing on plates: controlling guided waves using negative refraction. *Sci. Rep*. **5,** 11112 (2015).
36. Paniagua-Dominguez, R., Abujetas, D. R. & Sanchez-Gil, J. A. Ultra low-loss, isotropic optical negative-index metamaterial based on hybrid metal-semiconductor nanowires. *Sci. Rep*. **3,** 1507 (2013).
37. Bi, K. *et al.* Negative and near zero refraction metamaterials based on permanent magnetic ferrites. *Sci. Rep*. **4,** 4139 (2014).
38. Pendry, J. B., Schurig, D. & Smith, D. R. Controlling electromagnetic fields. *Science* **312,** 1780–1782 (2006).
39. Schurig, D. *et al.* Metamaterial electromagnetic cloak at microwave frequencies. *Science* **314,** 977–980 (2006).
40. Huang, Y. & Gao, L. Equivalent permittivity and permeability and multiple Fano resonances for nonlocal metallic nanowires. *J. Phys. Chem. C* **117,** 19203–19211 (2013).

41. Droulias, S. & Yannopapas, V. Broad-band giant circular dichroism in metamaterials of twisted chains of metallic nanoparticles. *J. Phys. Chem. C* **117,** 1130–1135 (2013).
42. Xue, H. J., Wu, R. L. & Yu. Y. Abnormal absorption and energy flow of electromagnetic wave in ultrathin metal films. *J. Phys. Chem. C* **118,** 18257–18262 (2014).
43. Yannopapas, V. & Psarobas, I. E. Ordered arrays of metal nanostrings as broadband super absorbers. *J. Phys. Chem. C* **116,** 15599–15603 (2012).
44. Zhang, F. *et al.* Microwave Conference, 2008. EuMC 2008. 38th European 2008; Vol. *1*, 801–804.
45. Kaelberer, T., Fedotov, V. A., Papasimakis, N., Tsai, D. P. & Zheludev, N. I. Toroidal dipolar response in a metamaterial. *Science* **330,** 1510–1512 (2010).
46. Boddis, A. M. & Russell, D. A. Simultaneous development and detection of drug metabolites in latent fingermarks using antibody-magnetic particle conjugates. *Anal. Methods* **31,** 519–523 (2011).
47. Groeneveld, G., de Puit, M., Bleay, S., Bradshaw, R. & Francese, S. Detection and mapping of illicit drugs and their metabolites in fingermarks by MALDI MS and compatibility with forensic techniques. *Sci. Rep.* **5,** 11716 (2015).
48. Wei, T. T. *et al.* Metabonomic analysis of potential biomarkers and drug targets involved in diabetic nephropathy mice. *Sci. Rep.* **5,** 11998 (2015).
49. Dong, W. B., Wu, R. B., Yuan, X. H., Li, C. W. & Tarn, T.-J. The modelling of quantum control systems. *Sci. Bull.* **60,** 1493 (2015).
50. Shen, Y., Ko, H.-Y., Ai, Q., Peng, S.-M. & Jin, B.-Y. Molecular split-ring resonators based on metal string complexes. *J. Phys. Chem. C* **118,** 3766–3773 (2014).
51. Libit, L. & Hoffmann, R. Toward a detailed orbital theory of substituent effects: charge transfer, polarization, and the methyl group. *J. Am. Chem. Soc.* **96,** 1370–1383 (1974).
52. Hoffmann, R. An extended Hückel theory. I. hydrocarbons. *J. Chem. Phys.* **39,** 1397–1412 (1963).
53. Hoffmann, R. Extended Hückel theory. III. compounds of boron and nitrogen. *J. Chem. Phys.* **40,** 2474–2480 (1964).
54. Hoffmann, R. Extended Hückel theory. IV. carbonium ions. *J. Chem. Phys.* **40,** 2480–2488 (1964).
55. Salem, L. *The molecular orbital theory of conjugated systems* (W. A. Benjamin, New York, 1966).
56. Hawkea, L., Kalosakasa, G. & Simserides, C. Empirical LCAO parameters for pi molecular orbitals in planar organic molecules. *Mol. Phys.* **107,** 1755–1771 (2009).
57. Harrison, W. A. *Electronic structure and the properties of solids* 2nd edn (Dover, New York, 1989).
58. Harrison, W. A. *Elementary electronic structure* (World Scientific, New Jersey, 1999).
59. NIST Chemistry Webbook and references therein. Available at: http://webbook.nist.gov/chemistry/. (Accessed: 4th December 2015).
60. Tokuji, S. A. *et al.* Facile formation of a benzopyrane-fused [28] hexaphyrin that exhibits distinct Möbius aromaticity. *J. Am. Chem. Soc.* **131,** 7240–7241 (2009).

Acknowledgements

The research was supported by Open Research Fund Program of the State Key Laboratory of Low-Dimensional Quantum Physics, Tsinghua University Grant No. KF201502. QA was also supported by the National Natural Science Foundation of China under Grant No. 11505007, and the Youth Scholars Program of Beijing Normal University under Grant No. 2014NT28.

Author Contributions

Y.S. wrote the main manuscript text and did the calculations. Y.S. and Q.A. designed the project and reviewed the manuscript.

Additional Information

Competing financial interests: The authors declare no competing financial interests.

How to cite this article: Shen, Y. and Ai, Q. Optical properties of drug metabolites in latent fingermarks. *Sci. Rep.* **6**, 20336; doi: 10.1038/srep20336 (2016).